Journal of Alloys and Compounds, 211/212 (1994) 625–627
JALCOM 151

Determination of ultrasonic attenuation in small samples of solid material by scanning acoustic microscopy with phase contrast

K. Hillmann and W. Grill
Physikalisches Institut, Johann Wolfgang Goethe-Universität, Robert-Mayer-Strasse 2-4, D-60 054 Frankfurt am Main (Germany)

J. Bereiter-Hahn
Arbeitskreis für kinematische Zellforschung, Zoologisches Institut, Johann Wolfgang Goethe-Universität, D-60 054 Frankfurt am Main (Germany)

Abstract

The attenuation of solid material or droplets of viscous liquids deposited on planar substrates is measured in the frequency regime from 300 MHz to 1.2 GHz by scanning acoustic microscopy with phase contrast. The observed spatial variations of the phases and amplitudes of the ultrasonic waves reflected from the objects contain sufficient information to determine the attenuation and velocity of ultrasonic waves in acoustically isotropic samples of minimal thickness about 1 μm and lateral extension down to 10 μm. The basic principles are discussed and an approximate treatment is presented together with typical results.

Scanning acoustic microscopy with phase contrast (PSAM) is used to determine the spatial dependences of the amplitudes and phases of the reflected ultrasonic waves of small samples (droplets) of solid or liquid material deposited on planar substrates (Fig. 1). The spatial dependence of the amplitudes reveals variations caused by interferences of the ultrasonic waves reflected from the surface of the sample and the interface to the substrate and multiple reflections within the sample [1]. The phase signal contains additional information which is employed together with the observed amplitudes to determine the mechanical properties of the samples.

For a planar substrate adjusted parallel to the scanning plane and a homogeneous sample with a sufficiently small tilting angle of the surface with respect to the sample–substrate interface (shallow droplets), the relevant content of the double image (Fig. 1) can be represented by a polar diagram of amplitudes and phases of the reflected ultrasonic waves (Fig. 2; the lower half of the polar representation is omitted in the figures presented here). Under these conditions the uncovered surface of the substrate is represented by a single point whereas the sample is represented by a spiral-shaped line. Each point of the spiral corresponds to the data for all points of equal thickness of the sample. The representation of the data in a polar diagram has the advantage that the four-dimensional representation (phases and amplitudes in the two dimensions of the image plane) is reduced to a curved line in two dimensions, which does not depend on the specific shape of the sample. The information contained in the measured polar diagram is the basis for the subsequent determination of the mechanical properties (velocity and attenuation of longitudinal ultrasonic waves and density) of the sample material.

For an illustration of the basic principle, a planar wave at normal incidence to a plane parallel sample with variable thickness deposited on a substrate is considered. The resulting calculated dependences of phases and amplitudes of the reflected ultrasonic waves show a distinct dependence on velocity (rotation) and attenuation (radial reduction) for increasing thickness of the sample. The shape of the loops is influenced by the reflectivity at the interfaces and therefore depends partly on the density of the sample. To describe the actual experimental conditions, the model calculations have been refined to include the influence of the angular spectrum of ultrasonic waves generated and detected by the ultrasonic lens system [2]. Depending on the thickness of the sample, this leads to alterations in the calculated polar diagrams with respect to the plane wave approximation. The main effect is a somewhat less pronounced interference structure caused by the integration over the different components of the angular spectrum. This model has been used to determine the mechanical properties of the samples by a procedure based on the variation of velocity, attenuation and density of the sample for an optimum fit of the calculated

SSDI 0925-8388(94)00151-2

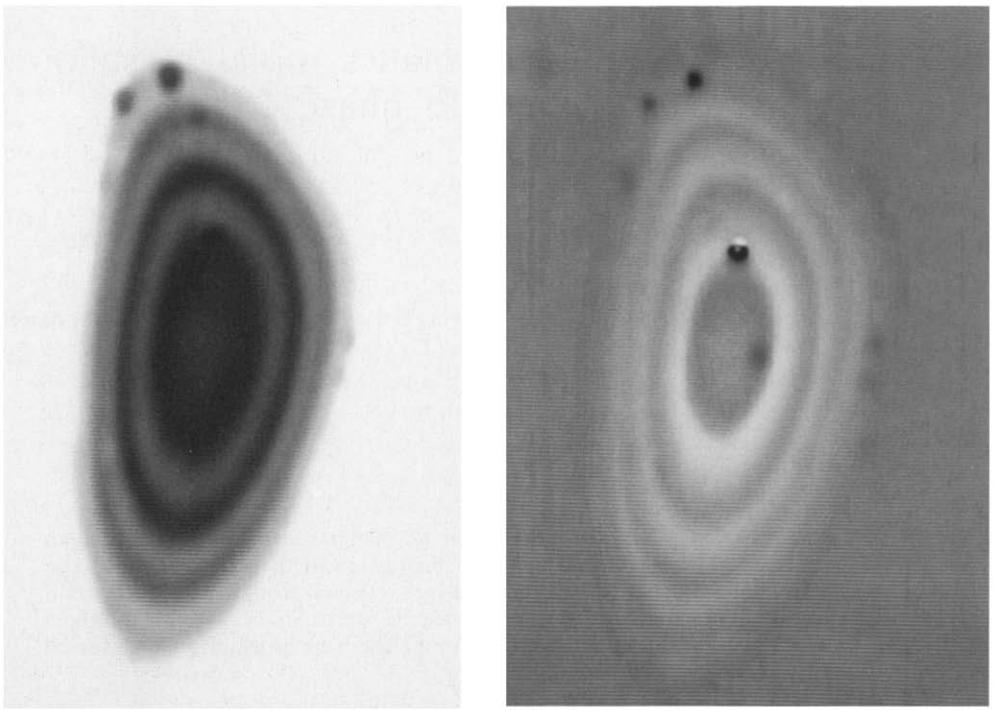

Fig. 1. PSAM images of amplitudes (left) and phases (right) at 1 GHz of a wax droplet deposited on a glass substrate with water at 22 °C as a coupling fluid. The grey scale of the phase image is proportional to the phase angle (black to white represents a phase angle of 0–2π); zero phase is chosen at an arbitrary angle. The scan range is 75 μm horizontally and 112 μm vertically.

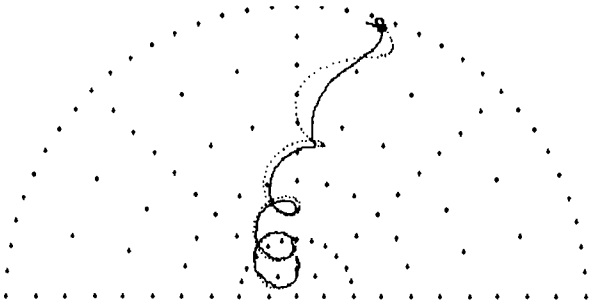

Fig. 2. Polar diagram of the amplitude (radial, arbitrary linear scale) *vs.* phase angle (circular, increasing clockwise) from the images in Fig. 1 (experimental data from a vertical line to the centre of the sample) and results of a model calculation (dotted line) including the influence of the angular spectrum with parameters of the sample chosen for optimum fit to the experimental results (velocity, 1542 m s^{-1}; attenuation, 3037 dB mm^{-1}; density, 0.863 g cm^{-3}).

polar diagram to the experimental results. A wax sample (droplet) deposited on a glass substrate has been chosen here to demonstrate the typical performance of this procedure (Fig. 2).

Good agreement is reached for the thicker parts of the sample, whereas only qualitative agreement is reached for the thin part of the sample. Owing to the droplet-like shape of the sample, the influence of the tilting angle of the surface of the sample material cannot be neglected close to the border line of the droplet, which is represented in the polar diagram by the outer part of the spiral. To correct for this effect, we have included a functional dependence of the reflection coefficient for the surface, approximating the reduced reflection caused by the tilt as expected from the observed topography of the sample (Fig. 1). This modification leads to a better fit of the model to the experimental results for the fraction of the polar diagram corresponding to the outer (thin) part of the droplet (Fig. 3).

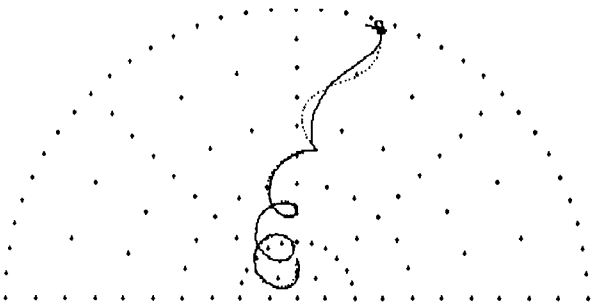

Fig. 3. Polar diagram of the experimental data and results of model calculations (dotted line) including the influence of the angular spectrum and the tilting of the surface of the sample with parameters of the sample chosen for optimum fit to the experimental results (velocity, 1542 m s^{-1}; attenuation, 2957 dB mm^{-1}; density, 0.863 g cm^{-3}).

For the given example (wax droplet on glass) the velocity of longitudinal ultrasonic waves can be determined by this procedure within an accuracy of 0.2%. Corresponding values for the attenuation coefficient are 1% and 0.5% for the density of the sample. Larger variations lead to clearly visible systematic deviations of the calculated polar diagram from the experimental results (apart from deviations for the thin part of the sample) which cannot be rectified by variations of the other adjustable parameters (examples of non-optimized fits are given in Figs. 4 and 5). The relevant parameters for the substrate (glass) were determined experimentally whereas the parameters for the coupling fluid (water) are selected according to the literature [3, 4].

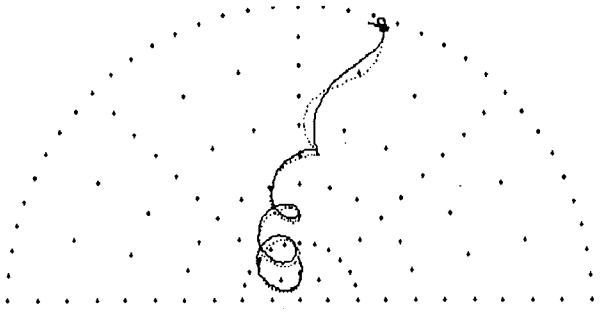

Fig. 4. Polar diagram of the experimental data and results of model calculations (dotted line) for an absorption coefficient 5% above the value for optimum fit to the experimental curve (other parameters as in Fig. 3).

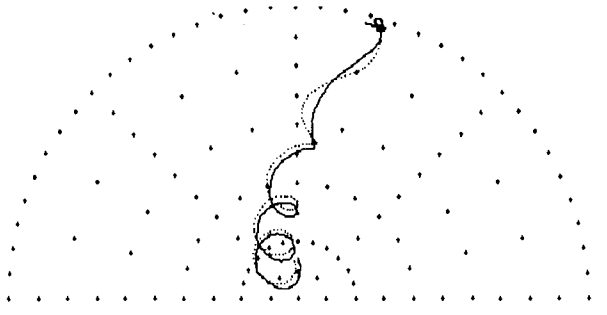

Fig. 5. Polar diagram as in Fig. 3 but for an absorption coefficient 5% below the value for optimum fit to the experimental curve.

The method has also been used to determine the mechanical properties of droplets of viscous liquids and living cells on various substrates with comparable resolution for samples of similar size. The model calculations presented here do not include the influence of surface waves, mode conversion to transverse modes (only of minor influence for wax, viscous liquids or living cells) or attenuated shear waves in viscous liquids. In the model calculations the angular spectrum has been chosen for best representation of the experimental results (gaussian distribution of the amplitude of the angular spectrum with a full width at half-maximum of 0.16π and constant phase in the focal plane). A further refinement of the model calculations can be achieved by the inclusion of the observed angular spectrum of the ultrasonic lenses as determined by independent measurements. Our current efforts are directed to achieve an even better fit to the experimental results by including these corrections and experimentally determined parameters of the angular spectrum of the lens system in the model calculations.

Acknowledgment

We would like to acknowledge support by the Deutsche Forschungsgemeinschaft.

References

1 J. Litniewski and J. Bereiter-Hahn, *J. Microsc., 158* (1990) 95.
2 K.K. Liang, G.S. Kino and B.T. Khuri-Yakub, *IEEE Trans. Sonics Ultrason., 32* (1985) 213.
3 W. Kroebel and K.-H. Mahrt, *Acoustica, 35* (1976) 154.
4 R.A. Lemons and C.F. Quate, in W.P. Mason and R.N. Thurston (eds.), *Physical Acoustics,* Vol. XIV, Academic Press, New York, 1979, p. 1.